

Structure-Activity Relationship Studies of Hydantoin-Cored Ligands for Smoothened Receptor

Yang Liu^{+, [a]}, Fang Zhou^{+, [a]}, Kang Ding^{+, [a]}, Dongxiang Xue^{+, [a]}, Zhihao Zhu^{+, [b]}, Cuixia Li^{+, [a, c]}, Fei Li^{+, [a]}, Yueming Xu^{+, [a]}, Fei Xu^{+, [a, c]}, Zhiping Le^{+, [b]}, Suwen Zhao^{+, * [a, c]} and Houchao Tao^{+, * [a]}

An underside binding site was recently identified in the transmembrane domain of smoothened receptor (SMO). Herein, we report efforts in the exploration of new insights into the interactions between the ligand and SMO. The hydantoin core in the middle of the parent compound was found to be highly conservative in chirality, ring size, and substituents. On each benzene at two ends, a plethora of variations, particularly halogen substitutions, were introduced and investigated. Analysis of the structure-activity relationship revealed miscellaneous halogen effects. The ligands with double halogen substituents exhibit remarkably enhanced potency, providing promising candidates that potentially overcome the common drug resistance and useful heavy-atom labeled chemical tools for co-crystallization studies of SMO.

1. Introduction

Hedgehog (Hh) signaling transduction is an evolutionarily conserved pathway that plays an essential role in embryonic and stem cell development.^[1] This pathway is initiated by the binding of Hh ligands to a 12- α -helix transmembrane protein Patched 1, which thereby activates a 7- α -helix transmembrane protein, smoothened receptor (SMO). The signal is then relayed to cytoplasm and induces subsequent gene transcription.^[2] In adult tissues, the Hh pathway generally maintains low activity.

However, abnormal continuous activation of this pathway has been related to several human cancers.^[3] Regulation of the Hh pathway has been an important pharmaceutical approach in the development of anti-cancer reagents.^[4] Specifically, many small molecules, either endogenous or synthetic ligands, have been uncovered, validated, and optimized.^[5] For example, three antagonist ligands targeting SMO, vismodegib (GDC-0449),^[6] sonidegib (LDE-0225),^[7] and glasdegib were marketed in 2012, 2015, and 2018 respectively, for the treatment of basal cell carcinoma and acute myeloid leukemia.^[8]

However, drug-resistant mutants of SMO often occurred after the clinical applications of these antagonists.^[9] For example, the D473H mutant showed much attenuated binding with vismodegib. Additionally, severe side effects, such as constipation, appetite loss, and muscle spasms, that limit clinical treatment of the above drugs to adult patients only have also been observed.^[10] Therefore, new molecules are urgently needed to combat drug resistance and extend biological applications in SMO.^[5e,11]

Lately, remarkable progress has been made in the structural studies of SMO, including its transmembrane domain (TMD), extracellular domain (ECD), and the multi-domain structures.^[12] In these high-resolution structures, the contacts of SMO with many bound ligands, including LY2940680 (taladegib),^[13] SAG, ANTA-IV, SANT-1, cyclopamine,^[14] TC-114,^[15] and vismodegib^[16] in the traditional TMD binding site were precisely described. Using photoaffinity labeling and computational technology, our group recently explored the binding mechanism of Allo-1.^[17] Allo-1 occupies a narrow and deep site beneath the canonical TMD binding that is far away from the most common mutation D473H (Figure 1). The distinct binding of Allo-1 makes it promising in battling drug-resistant SMO mutants. Focusing on Allo-1, we conducted a comprehensive investigation of the structure-activity relationship from which new insights were revealed and ligands with enhanced potency were obtained.

2. Results and Discussion

2.1. Design of Allo-1 Analogs

The parent Allo-1 was first structurally divided into three parts: a central hydantoin core, an upper aniline benzene, and a lower benzyl benzene, as illustrated in Figure 1C. The central hydantoin core is frequently found in clinical pharmaceuticals.^[18] A previous investigation revealed that the two carbonyl oxygens undergo hydrogen bonding with

[a] Dr. Y. Liu,⁺ Dr. F. Zhou,⁺ K. Ding,⁺ Dr. D. Xue, C. Li, F. Li, Dr. Y. Xu, Prof. F. Xu, Prof. S. Zhao, Prof. H. Tao
iHuman Institute
ShanghaiTech University
393 Middle Huaxia Road, Shanghai 201210 (China)
E-mail: zhaosw@shanghaitech.edu.cn
taohch@shanghaitech.edu.cn

[b] Z. Zhu, Prof. Z. Le
Department of Chemistry
Nanchang University
999 Xuefu Avenue, Nanchang 330031 (China)

[c] C. Li, Prof. F. Xu, Prof. S. Zhao
School of Life Science and Technology
ShanghaiTech University
393 Middle Huaxia Road, Shanghai 201210 (China)

[†] These authors contributed equally to this work.

Supporting information for this article is available on the WWW under <https://doi.org/10.1002/open.202100216>

© 2021 The Authors. Published by Wiley-VCH GmbH. This is an open access article under the terms of the Creative Commons Attribution Non-Commercial NoDerivs License, which permits use and distribution in any medium, provided the original work is properly cited, the use is non-commercial and no modifications or adaptations are made.

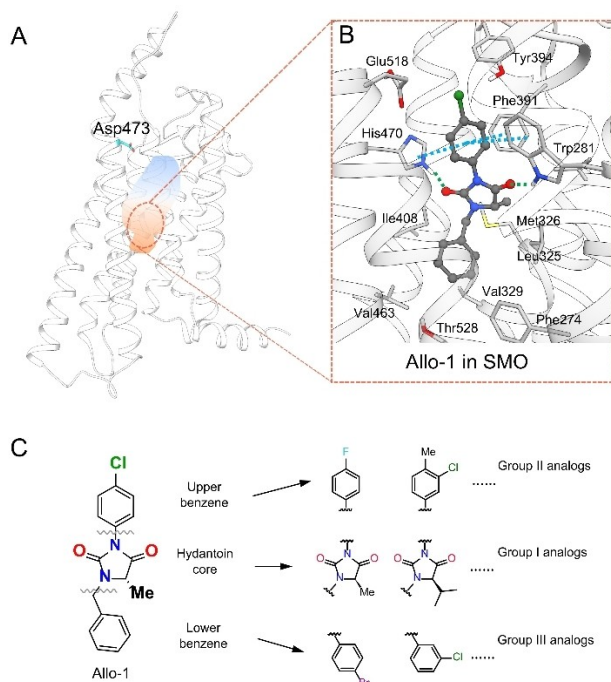
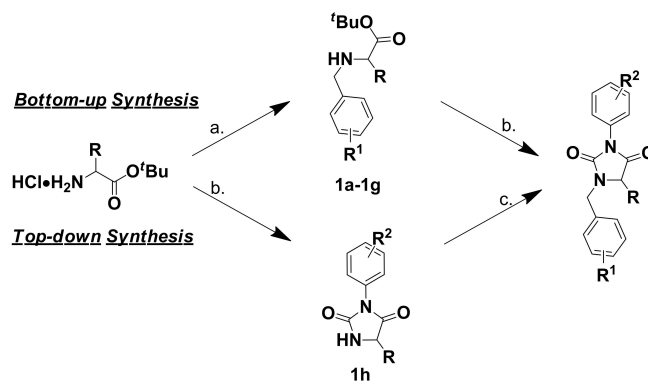


Figure 1. Computation-guided design of Allo-1 analogs that occupy the underside binding site of SMO. (A) Allo-1 binding is far away from the common drug resistance mutation Asp473. (B) Key interactions identified for Allo-1 binding. (C) Three groups of analogs designed by the dissection of the Allo-1 structure.

residues Trp281 and His470, respectively.^[17b] These residues distinguished Allo-1 from other molecules in this binding and provided clues on what to retain. Group I analogs were then designed to explore the chirality and size of substitution on hydantoin. The upper benzene ring of aniline, which is tightly captured by a π -cage surrounded by residues Trp281, Phe391, and His470, was crucial for the binding. Strong π - π interactions were observed among these residues. Group II analogs with various substituents were proposed to strengthen interactions within this π -cage. The lower benzene ring of Allo-1 appears to be involved in hydrophobic interactions within a hydrophobic crevice only. The only polar residue at the bottom of the binding site, Thr528, may be utilized to establish a polar interaction. Actually, the Allo-2 binding that has previously been predicted does indeed consist of a hydrogen bond between its indazole group and Thr528 (Figure S1, Supporting Information).^[17a] Group III analogs were therefore designed for verification.

2.2. Synthesis of Allo-1 Analogs

In principle, Allo-1 and its analogs can be synthesized using two convergent approaches, as summarized in Scheme 1. The first synthetic approach is the bottom-up strategy. Under this strategy, amino esters are first alkylated with benzyl bromides for the lower benzene portion of Allo-1 analogs. Then, the resulting *N*-benzyl amino *t*-butyl esters are conjugated with aryl



Scheme 1. Reagents and conditions: a. benzyl bromide, DIPEA, CH₃CN; b. i. 4-chlorophenyl isocyanate, CH₃CN, r.t., overnight; ii. 12 M HCl, r.t., 10 h; c. benzyl bromide, Cs₂CO₃, CH₃CN.

isocyanate, followed by acidification-promoted cyclization that affords the hydantoin core. Group I compounds were prepared from different amino esters (Scheme S1). This approach was also applied to synthesize group II analogs, thus facilitating the derivation of the upper benzene ring with a variety of substituted phenyl isocyanates after acidification and other functional group transformations, if needed (Scheme S2). The second synthetic approach to obtain Allo-1 and its analogs is the top-down strategy. Under this strategy, the upper benzene group is first obtained by building the hydantoin core using phenyl isocyanates and the unsubstituted (*S*)-alanine *t*-butyl ester.^[19] Group III compounds were then prepared by *N*-alkylation of the hydantoin with various benzyl halides (Scheme S3). Double halogen-incorporating compounds were synthesized using the same method as group II ligands (Scheme S4). Analogues with hydroxyl or amine substitution were obtained from one more reduction step from benzyl ether or nitro compounds (Scheme S5). Overall, the synthesis of Allo-1 and its analogs can be conveniently achieved by the above-detailed two-pot three-step procedures with the various amino esters, aryl bromides, and aryl isocyanates, respectively.

2.3. Inhibition of Analogs to the Hh Pathway

Evaluation of Group I analogs suggested that the hydantoin core, (*S*)-5-methylimidazolidine-2,4-dione, is highly conserved in the tight-binding within this underside site (Table 1). Previous studies indicated that the hydantoin core is responsible for the tight-binding of Allo-1 (Figure 1B, Figure S2A). To investigate the chirality of Allo-1, which was not previously known, an explicit pair of chiral compounds (Figure S3, Table S1), namely, (*S*)-Allo-1 (**2a**) and (*R*)-Allo-1 (**2b**), were compared. An activity difference of approximate threefold was observed between the enantiomeric pair, and the (*S*)-isomer was more potent than the (*R*)-isomer. A docking study of **2b** indicated that the twisting angle of hydantoin blocks hydrogen bonding with Trp281 (Figure S2B). Increasing the size of the side chain, as in both (*S*)- and (*R*)-isopropyl derivatives (**2c** and **2d**), only led to a complete loss of activity. Even in the (*S*)-configuration, a slight

Table 1. Inhibition of the Hh pathway by Group I analogs.			
	R =	Compds.	IC ₅₀ ^[a] [nM]
	Me (<i>S</i>)	Allo-1 (2a)	81.8 ± 19.4
	Me (<i>R</i>)	2b	198.7 ± 57.2
	<i>i</i> -Pr (<i>S</i>)	2c	> 10000
	<i>i</i> -Pr (<i>R</i>)	2d	> 10000
	Et (<i>S</i>)	2e	389.4 ± 22.1
	H	2f	958.8 ± 144.2
	Me ₂	2g	> 10000
		2h	> 10000
		2i	> 10000

[a] IC₅₀ of luciferase reporter assay represents the mean ± SEM of three independent experiments carried out in duplicate.

increase in substitution from methyl (**2a**) to ethyl (**2e**) suppressed the activity to one fifth the original activity (Figure S2C). Docking studies of the (*S*)-isopropyl derivative (**2c**) showed a severe hindrance blocking all interactions, including hydrogen bonding and π -cage trapping (Figure S2D). Removal of methyl (**2f**) also resulted in over 90% reduction in activity (Figure S2E). The *gem*-substituted analog (**2g**) showed remarkably reduced activity, thereby indicating over-crowding. Other attempts towards the modification of the scaffold consistently yielded severely impaired ligands. For example, only inactive compounds were generated after ring expansion from the 5-membered imidazolidine-1,3-dione to the 6-membered pyrimidine-2,4-dione (**2h**) and ring fusion of benzyl with hydantoin (**2i**) for conformation locking (Figure S4). Hence, the core structure of Allo-1 specifically interacts with the receptor and is highly sensitive even to slight modification. This sensitivity is also reflected in the change of free energy binding (Table S2).^[20]

In the evaluation of Group II analogs (Table 2), a likely halogen-bond effect was first observed among the 4-halogen substituted homolog series (**2a**, **3a–3d**, Figure 2A).^[21] 4-F analog **3b** exhibited considerably lower activity than the original 4-Cl Allo-1 (**2a**). By contrast, the activities of the 4-Br

Table 2. Inhibition of the Hh pathway by Group II analogs.			
	R =	Compds.	IC ₅₀ ^[a] [nM]
	4-Cl	Allo-1 (2a)	81.8 ± 19.4
	4-H	3a	379.3 ± 9.5
	4-F	3b	521.1 ± 141.1
	4-Br	3c	19.6 ± 4.0
	4-I	3d	19.1 ± 6.8
	4-Me	3e	64.3 ± 14.4
	4-CF ₃	3f	19.5 ± 7.9
	3-F	4a	238.3 ± 14.1
	3-Cl	4b	117.4 ± 18.5
	3-Br	4c	57.7 ± 18.0
	3-I	4d	54.0 ± 27.6
	3,4-Cl ₂	4e	52.6 ± 27.1
	3-Cl, 4-Me	4f	15.3 ± 0.4
	4-NH ₂	5a	237.5 ± 40.1
	4-COOMe	5b	> 10000
4-OH	5c	48.8 ± 3.5	

[a] IC₅₀ of luciferase reporter assay represents the mean ± SEM of three independent experiments carried out in duplicate.

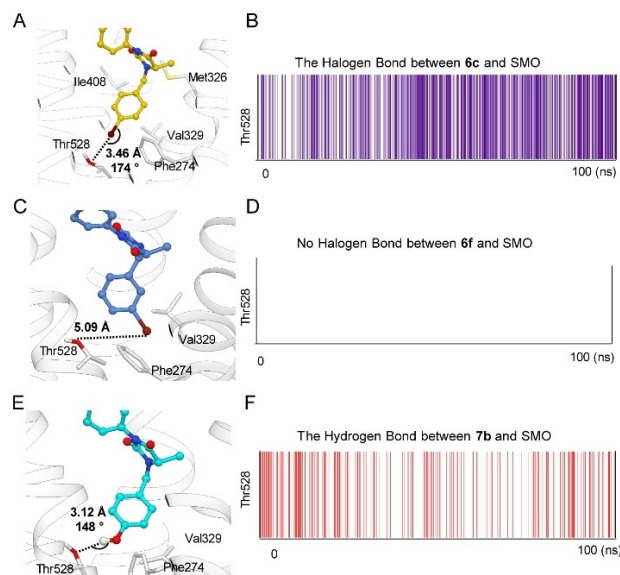


Figure 2. Bottom halogen bond between 4-halogen substituents and Thr528. (A) 4-Br-substituted analog **6c** forms a halogen bond with Thr528 on account of their acceptable distance and angle. (B) The results of 100 ns simulations showed continuous interactions between **6c** and Thr528. (C) 3-Br substituted analog **6f** showed unfavored halogen bond interaction, as indicated in the simulation results (D) due to the improper distance and angle. (E) 4-OH substituted analog **7b** can form a considerable hydrogen bond interaction with Thr528 in the simulation results (F).

and 4-I analogs (**3c** and **3d**) improved by four-fold. Removal of 4-Cl from Allo-1, such as in compound **3a** (4-H), led to an 80% reduction in activity, again confirming the significant contribution of 4-Cl to this binding. In a 100 ns simulation, an interaction between Glu518 and 4-Cl in Allo-1 was observed at only a few percent (Figure S5), probably indicating a weak halogen bond. However, the halogen dependent effect could possibly also be ascribed to the increasing hydrophobic effect. Indeed, the halogen bioisostere-substituted analogs, such as **3e** (4-Me) and **3f** (4-CF₃), also exhibited enhanced activities, suggesting a more important role of the hydrophobic over the halogen bond effect in this context.

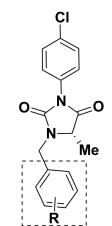
Similarly, evaluation of the 3-halogen substituted compounds (**4a–4d**) also indicated a possible trend of classic halogen bonding (3-F (**4a**) > 3-Cl (**4b**) > 3-Br (**4c**) ≈ 3-I (**4d**), Table 2), albeit with slightly weaker potency when compared with that of their 4-substituted counterparts. In a 100 ns simulation of the 3-Cl analog (**4b**), the interaction between the 3-Cl substituent and Tyr394 was observed (Figure S6), instead of that between 4-Cl and Glu518. Notably, the effects of the two substituents seem to be compatible, as analogs **4e** (3,4-Cl₂) and **4f** (3-Cl, 4-Me) are further improved when compared with the other two mono-substituted analogs (i.e. **4b**, **3e** and Allo-1, Table 2).

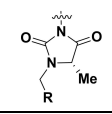
In addition, the establishment of hydrogen bonding was also investigated in this context (Table 2). The 4-OH analog (**5c**) was more potent than the 4-H analog (**3a**) and even the 4-Cl parent compound Allo-1, indicative of hydrogen bonding in this context (Figure S7). In comparison, the 4-NH₂ (**5a**) and 4-carboxylate (**5b**) analogs were less active, in which the hydro-

gen bond would probably be offset by weakened π -cage interactions due to the reduction in electron density brought about by the positively charged 4-NH₂ or electron-withdrawing carboxylate substituents. This observation is in agreement with the presence of hydrogen bonding and non-weakened π -interactions. Relevantly, halogen substituents, especially Br and I, appear to be relatively neutral and non-harmful for the established π -interaction.

Group III analogs were evaluated to explore the possibility to strengthen the binding by using Thr528 in the lower binding area. As shown, the 4-halogen introduction at the bottom benzene indeed improved the activities, including the 4-F analog (**6a**) and even the 2,4-F₂ analog (**6e**) (Table 3). The activities followed a classical trend of halogen bonding. Among these compounds, the 4-Br analog (**6c**) was most potent with a single-digit nanomolar activity. The 4-I analog (**6d**) showed only half the activity of **6c**, probably reflecting a strict steric interaction. The participation of Thr528 in the continuous interaction with 4-Br in **6c** has been confirmed by docking and simulation studies (Figure 2A–B, Figure S8). As shown, 4-Br is close to Thr528 in an appropriate angle, in agreement to the requirement of halogen bonding. Actually, the distance and the angle are crucial for such a halogen bond. As a sharp comparison to 4-Br analog (**6c**), the 3-Br analog (**6f**) exhibited a much attenuated activity (IC₅₀ 503 nM vs. 9.3 nM) due to its unmatched orientation for the establishment of halogen bonding. Correspondingly, no interaction between 3-Br and Thr528 was observed in the simulation study (Figure 2C–D, Figure S9). Nevertheless, the hydrophobic effect was also not excluded. When halogen bioisosteres were introduced, such as 4-Me (**6g**) and 4-CF₃ (**6h**), the potencies were comparable to the 4-halogen analogs (Table 3). The drastic decrease in activity of analog **6i** (4-*t*-Bu) was in good agreement to **6d** (4-I), again indicative of steric interaction.

Table 3. Inhibition of the Hh pathway by Group III analogs.			
R=	Compds.	IC ₅₀ ^[a] [nM]	
4-H	Allo-1	81.8 ± 19.4	
4-F	6a	35.9 ± 10.8	
4-Cl	6b	19.5 ± 7.9	
4-Br	6c	9.3 ± 5.1	
4-I	6d	20.3 ± 6.2	
2,4-F ₂	6e	57.1 ± 11.3	
3-Br	6f	505.6 ± 24.2	
4-Me	6g	16.74 ± 2.9	
4-CF ₃	6h	17.0 ± 2.2	
4- <i>t</i> -Bu	6i	1592 ± 169.8	
4-NH ₂	7a	917.5 ± 121.4	
4-OH	7b	183.7 ± 33.7	
4-NO ₂	7c	204.6 ± 23.1	
4-CN	7d	721.5 ± 94.9	
4-SO ₂ Me	7e	> 10 000	
4-CO ₂ Me	7f	585.2 ± 225.5	
2-Pyridyl	8a	> 10 000	
3-Pyridyl	8b	> 10 000	
4-Pyridyl	8c	> 10 000	





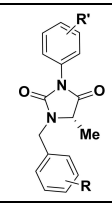
[a] IC₅₀ of luciferase reporter assay represents the mean ± SEM of three independent experiments carried out in duplicate.

On the other hand, we also attempted establishing hydrogen bonding between Thr528 and the ligands. To this end, substitutions at the lower benzene ring were introduced in the form of the hydrogen donors 4-NH₂ (**7a**) and 4-OH (**7b**) as well as with acceptor groups 4-SO₂Me (**7c**), 4-CO₂Me (**7d**), 4-CN (**7e**), and 4-NO₂ (**7f**). Alternatively, the lower benzene ring was replaced with a pyridyl group (**8a–8c**). Unexpectedly, all these purposely designed compounds exhibited no improvement over the parent Allo-1. Even the best analog, 4-OH substituted (**7b**), exhibited a two-fold reduced activity over Allo-1 and a 20-fold reduction over 4-Br analog (**6c**), although the establishment of a hydrogen bond between Thr528 and 4-OH was clearly confirmed by the considerable interactions observed in the simulation study (Figure 2E–F, Figure S10). We speculate that the ineffectiveness of hydrogen bonding in this context is complicated by the enthalpy penalty during solvation/desolvation of the ligands with polar groups.^[22]

Finally, with the retained 4-Br in the lower benzene group, compounds (**9a–9b**) paired with 4-Br and 4-I in the upper benzene ring, respectively, maintained their high activity (Table 4), which was however slightly lower than that of their 4-Cl analog (**6c**). It seems to be difficult to perfectly accommodate both halogen substituents simultaneously and maximize the activity enhancement due to the strict requirement of bond distance and bond angle. Meanwhile, the steric interaction also affects the proper introduction of suitably sized halogen atoms. Nevertheless, we achieved an about nine-fold enhancement in activity for future pharmaceutical application (**6b–6c**) and obtained doubly heavy atom labelled ligands (**9a–9b**) for co-crystallization studies of SMO.

3. Conclusion

In summary, we successfully obtained ligands with enhanced activity for SMO by the rational introduction of halogen substituents. Halogen atoms are commonly found in clinical drugs. Their role has been well documented in the adjustment of steric hindrance, metabolism, and lipophilicity.^[23] In this study, we systematically investigated the halogen effects of the ligands that probably resulted from miscellaneous interactions, including halogen bonding and hydrophobic effects. The resulting double halogen-bonded compounds exhibited consid-

Table 4. Double halogen bond-enhanced analogs for inhibition of the Hh pathway.				
	R=	R' =	Compds.	IC ₅₀ ^[a] [nM]
	4-H	4-H	3a	379.3 ± 9.5
	4-H	4-Cl	Allo-1	81.8 ± 19.4
	4-Cl	4-Cl	6b	19.5 ± 7.9
	4-Br	4-Cl	6c	9.3 ± 5.1
	4-Br	4-Br	9a	15.3 ± 0.4
	4-Br	4-I	9b	14.4 ± 2.9

[a] IC₅₀ of luciferase reporter assay represents the mean ± SEM of three independent experiments carried out in duplicate.

erably improved activity in the antagonism towards SMO. The analysis of the structure-activity relationship verified the accuracy of Allo-1 binding. Furthermore, these properly halogenated ligands also offer reliable fiducials that facilitate the phase determination in crystallography studies. A co-crystallization study of the selected ligands from this study, as well as other halogenated ligands obtained by similar strategies, is ongoing in our laboratory and will be reported in due course.

Experimental Section

See the Supporting Information for general experimental information, standard procedures, spectral data, characterization, luciferase reporter assay, and copies of spectra of the prepared compounds.

Acknowledgements

The authors (S.Z. and H.T.) are thankful to Shanghai Municipal Government, ShanghaiTech University, GPCR Consortium, and National Key R&D Program of China (2018YFA0507000) for support. We thank Q. Shi, Q. Tan, J. Liu and L. Yang for assistance in the membrane preparation, plasmid preparation and NMR data collection respectively at the Core Facility of iHuman Institute. We thank Y. Zhao for the generous donation of NIH-3T3 cell line for the assay.

Conflict of Interest

The authors declare no conflict of interest.

Keywords: anti-cancer · halogen bonding · molecular dynamics · smoothened receptor · structural biology

- [1] J. Briscoe, P. P. Therond, *Nat. Rev. Mol. Cell Biol.* **2013**, *14*, 416–429.
- [2] A. M. Arensdorf, S. Marada, S. K. Ogden, *Trends Pharmacol. Sci.* **2016**, *37*, 62–72.
- [3] a) M. P. di Magliano, M. Hebrok, *Nat. Rev. Cancer* **2003**, *3*, 903–911; b) J. Jiang, C.-c. Hui, *Dev. Cell* **2008**, *15*, 801–812.
- [4] L. L. Rubin, F. J. de Sauvage, *Nat. Rev. Drug Discovery* **2006**, *5*, 1026–1033.
- [5] a) F. Ghirga, M. Mori, P. Infante, *Bioorg. Med. Chem. Lett.* **2018**, *28*, 3131–3140; b) P. Heretsch, L. Tzagkaroulaki, A. Giannis, *Bioorg. Med. Chem.* **2010**, *18*, 6613–6624; c) G. Liu, J. Yang, J. Wang, X. Liu, W. Huang, J. Li, W. Tan, A. Zhang, *J. Med. Chem.* **2016**, *59*, 11050–11068; d) W. Lu, D. Zhang, H. Ma, S. Tian, J. Zheng, Q. Wang, L. Luo, X. Zhang, *Eur. J. Med. Chem.* **2018**, *155*, 34–48; e) L. Ye, K. Ding, F. Zhao, X. Liu, Y. Wu, Y. Liu, D. Xue, F. Zhou, X. Zhang, R. C. Stevens, F. Xu, S. Zhao, H. Tao, *MedChemComm* **2017**, *8*, 1332–1336; f) M. Xin, *Expert Opin. Ther. Pat.* **2015**, *25*, 549–565.
- [6] G. J. P. Dijkgraaf, B. Aliche, L. Weinmann, T. Januario, K. West, Z. Modrusan, D. Burdick, R. Goldsmith, K. Robarge, D. Sutherlin, S. J. Scales, S. E. Gould, R. L. Yauch, F. J. de Sauvage, *Cancer Res.* **2011**, *71*, 435–444.
- [7] S. Pan, X. Wu, J. Jiang, W. Gao, Y. Wan, D. Cheng, D. Han, J. Liu, N. P. Englund, Y. Wang, S. Peukert, K. Miller-Moslin, J. Yuan, R. Guo, M. Matsumoto, A. Vattay, Y. Jiang, J. Tsao, F. Sun, A. C. Pferdekemper, S. Dodd, T. Tuntland, W. Maniara, J. F. Kelleher, III, Y.-m. Yao, M. Warmuth, J. Williams, M. Dorsch, *ACS Med. Chem. Lett.* **2010**, *1*, 130–134.
- [8] a) E. Dolgin, *Nat. Med.* **2011**, *17*, 523; b) C. A. Maschinot, J. R. Pace, M. K. Hadden, *Curr. Med. Chem.* **2015**, *22*, 4033–4057; c) M. J. Munchhof, Q. Li, A. Shavnya, G. V. Borzillo, T. L. Boyden, C. S. Jones, S. D. LaGreca, L. Martinez-Alsina, N. Patel, K. Pelletier, L. A. Reiter, M. D. Robbins, G. T. Tkalcevic, *ACS Med. Chem. Lett.* **2012**, *3*, 106–111.
- [9] a) T. Brinkhuizen, M. G. Reinders, M. Van Geel, A. J. L. Hendriksen, A. D. C. Paulussen, V. J. Winnepenninckx, K. B. Keymeulen, P. M. M. B. Soetekouw, M. A. M. Van Steensel, K. Mosterd, *J. Am. Acad. Dermatol.* **2014**, *71*, 1005–1008; b) R. L. Yauch, G. J. P. Dijkgraaf, B. Aliche, T. Januario, C. P. Ahn, T. Holcomb, K. Pujara, J. Stinson, C. A. Callahan, T. Tang, J. F. Bazan, Z. Kan, S. Seshagiri, C. L. Hann, S. E. Gould, J. A. Low, C. M. Rudin, F. J. De Sauvage, *Science* **2009**, *326*, 572–574; c) T. W. Ridky, G. Cotsarelis, *Cancer Cell* **2015**, *27*, 315–316.
- [10] E. Pak, R. A. Segal, *Dev. Cell* **2016**, *38*, 333–344.
- [11] X. Dong, C. Wang, Z. Chen, W. Zhao, *Drug Discovery Today* **2018**, *23*, 704–710.
- [12] E. F. X. Byrne, G. Luchetti, R. Rohatgi, C. Siebold, *Curr. Opin. Cell Biol.* **2018**, *51*, 81–88.
- [13] C. Wang, H. Wu, V. Katritch, G. W. Han, X.-P. Huang, W. Liu, F. Y. Siu, B. L. Roth, V. Cherezov, R. C. Stevens, *Nature* **2013**, *497*, 338–343.
- [14] C. Wang, H. Wu, T. Evron, E. Vardy, G. W. Han, X.-P. Huang, S. J. Hufeisen, T. J. Mangano, D. J. Urban, V. Katritch, V. Cherezov, M. G. Caron, B. L. Roth, R. C. Stevens, *Nat. Commun.* **2014**, *5*, 4355.
- [15] X. Zhang, F. Zhao, Y. Wu, J. Yang, G. W. Han, S. Zhao, A. Ishchenko, L. Ye, X. Lin, K. Ding, V. Dharmarajan, P. R. Griffin, C. Gati, G. Nelson, M. S. Hunter, M. A. Hanson, V. Cherezov, R. C. Stevens, W. Tan, H. Tao, F. Xu, *Nat. Commun.* **2017**, *8*, 15383.
- [16] E. F. X. Byrne, R. Sircar, P. S. Miller, G. Hedger, G. Luchetti, S. Nachtergaele, M. D. Tully, L. Mydock-McGrane, D. F. Covey, R. P. Rambo, M. S. P. Sansom, S. Newstead, R. Rohatgi, C. Siebold, *Nature* **2016**, *535*, 517–522.
- [17] a) H. Tao, Q. Jin, D.-I. Koo, X. Liao, N. P. Englund, Y. Wang, A. Ramamurthy, P. G. Schultz, M. Dorsch, J. Kelleher, X. Wu, *Chem. Biol.* **2011**, *18*, 432–437; b) F. Zhou, K. Ding, Y. Zhou, Y. Liu, X. Liu, F. Zhao, Y. Wu, X. Zhang, Q. Tan, F. Xu, W. Tan, Y. Xiao, S. Zhao, H. Tao, *J. Med. Chem.* **2019**, *62*, 9983–9989.
- [18] L. Konnerth, F. Lamaty, J. Martinez, E. Colacino, *Chem. Rev.* **2017**, *117*, 13757–13809.
- [19] A. J. Bischoff, B. M. Nelson, Z. L. Niemeyer, M. S. Sigman, M. Movassaghi, *J. Am. Chem. Soc.* **2017**, *139*, 15539–15547.
- [20] J. Li, R. Abel, K. Zhu, Y. Cao, S. Zhao, R. A. Friesner, *Proteins Struct. Funct. Bioinf.* **2011**, *79*, 2794–2812.
- [21] Y. Lu, T. Shi, Y. Wang, H. Yang, X. Yan, X. Luo, H. Jiang, W. Zhu, *J. Med. Chem.* **2009**, *52*, 2854–2862.
- [22] a) J. Fanfrlik, M. Kolar, M. Kamlar, D. Hurny, F. X. Ruiz, A. Cousido-Siah, A. Mitschler, J. Rezac, E. Munusamy, M. Lepsik, P. Matejcek, J. Vesely, A. Podjarny, P. Hobza, *ACS Chem. Biol.* **2013**, *8*, 2484–2492; b) J. Fanfrlik, F. X. Ruiz, A. Kadlcikova, J. Rezac, A. Cousido-Siah, A. Mitschler, S. Haldar, M. Lepsik, M. H. Kolar, P. Majer, A. D. Podjarny, P. Hobza, *ACS Chem. Biol.* **2015**, *10*, 1637–1642.
- [23] G. Gerebtzoff, X. Li-Blatter, H. Fischer, A. Frenzel, A. Seelig, *Chem-BioChem* **2004**, *5*, 676–684.

Manuscript received: September 15, 2021

Revised manuscript received: September 16, 2021